PERGAMON

Journal of Asian Earth Sciences 19 (2001) 737–749

Journal of Asian Earth Sciences

www.elsevier.com/locate/jseaes

Polyphase Alpine deformation at the northern edge of the Menderes–Taurus block, North Konya, Central Turkey

Yasar Eren

Department of Geology, Selçuk University, Kampus, Konya, Turkey

Received 17 May 2000; accepted 29 December 2000

Abstract

Low-grade metamorphic rocks of Paleozoic–Mesozoic age to the north of Konya, consist of two different groups. The Silurian–Lower Permian Sizma Group is composed of reefal complex metacarbonates at the base, and flyschoid metaclastics at the top. Metaigneous rocks of various compositions occur as dykes, sills, and lava flows within this group. The ?Upper Permian–Mesozoic age Ardicli Group unconformably overlies the Sizma Group and is composed of, from bottom to top, coarse metaclastics, a metaclastic–metacarbonate alternation, a thick sequence of metacarbonate, and alternating units of metachert, metacarbonates and metaclastics. Although pre-Alpine overthrusts can be recognized in the Sizma Group, intense Alpine deformation has overprinted and obliterated earlier structures. Both the Sizma and Ardicli Groups were deformed, and metamorphosed during the Alpine orogeny. Within the study area evidence for four phases of deformation and folding is found. The first phase of deformation resulted in the major Ertugrul Syncline, overturned tight to isoclinal and minor folding, and penetrative axial planar cleavage developed during the Alpine crustal shortening at the peak of metamorphism. Depending on rock type, syntectonic crystallization, rotation, and flattening of grains and pressure solution were the main deformation mechanisms. During the F_2-phase, continued crustal shortening produced coaxial Type-3 refolded folds, which can generally be observed in outcrop with associated crenulation cleavage (S_2). Refolding of earlier folds by the noncoaxial F_3-folding event generated Type-2 interference patterns and the major Meydan Synform which is the largest map-scale structure within the study area. Phase 3 structures also include crenulation cleavage (S_3) and conjugate kink folds. Further shortening during phase 4 deformation also resulted in crenulation cleavage and conjugate kink folds. According to thin section observations, phases 2–4 crenulation cleavages are mainly the result of microfolding with pressure solution and mineral growth.

Keywords: Central Turkey; Alpine deformation; Polyphase folding; Crenulation cleavage

1. Introduction

The area investigated is located in Central Turkey, 20 km northwest of Konya (Fig. 1). According to the classical geotectonic classification of Ketin (1966), Turkey consists of four major belts from north to the south; the Pontides, the Anatolides, the Taurides and the Border folds. Sengör and Yilmaz (1981), Sengör et al. (1984) and Sengör (1984) classified the major tectonic elements of Turkey in terms of plate tectonics. According to these studies, the Rhodope–Pontide Fragment, Sakarya Continent, the Menderes–Taurus Block, the Kirsehir Block, and the suture zones between them, form the major paleotectonic elements of Turkey (Fig. 1). The Pontides, forming the northern part of Turkey, are separated from the other tectonic units by the Izmir–Ankara and Erzincan suture zones. Sengör (1984) divided the Pontides into the Sakarya Continent and the Rhodope–Pontide Fragment. According to Okay (1986), the Pontides consist of three major zones, namely the Istranca Massif, Istanbul and Sakarya zones. The Anatolides consist mainly of median crystalline massifs and exhibit strong Alpine metamorphism. Okay (1984, 1986) distinguished four major units in the Anatolides, the Afyon–Bolkardagi Zone, Tavsanli Zone, Menderes and Kirsehir massifs, and considered them as metamorphic equivalents of the Taurides. The Taurides are made up of imbricated nappes comprising mostly Paleozoic to Early Tertiary sedimentary rocks. Sengör (1984), considered the Anatolides and Taurides of Ketin (1966) as the Anatolide–Tauride Platform and divided it into the Menderes–Taurus Block and the Kirsehir Block, which are separated by the Inner Tauride Suture. The Border Folds represent the gently folded north-facing passive continental margin of the Arabian Platform. During the Mesozoic time, the Rhodope–Pontide Fragment, the Sakarya Continent, the Menderes–Taurus Block, and the Kirsehir Block were separated from each other by

E-mail address: erenyasar@hotmail.com (Yasar Eren).

1367-9120/01/$ - see front matter
PII: S1367-9120(01)00009-8

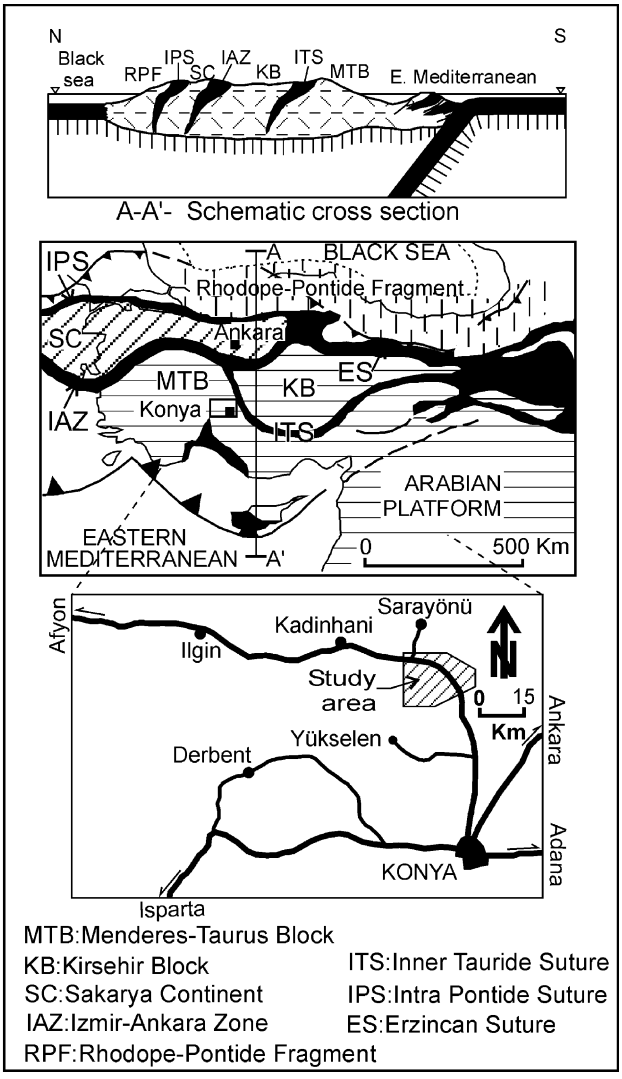

Fig. 1. Paleotectonic map of Turkey (Sengör et al., 1984) and the location of the study area.

narrow branches of Neo-Tethyan Ocean. The closure of these oceanic branches during the Early Tertiary, formed several suture zones (Fig. 1), which represent the Alpine orogeny in Turkey.

In this tectonic framework, the study area is situated on the northern edge of the Menderes–Taurus Block, approximately 50 km southwest of the Inner Tauride Suture Zone, and is included within the Alpine metamorphics of the Anatolides. The low-grade Paleozoic and Mesozoic metamorphic rocks of the study area belong to the Afyon–Bolkardagi Zone of Okay (1986) or the Kütahya–Bolkardagi Belt of Özcan et al. (1988).

Most of the early studies (Wiesner, 1968; Göger and Kiral, 1969) considered only the general stratigraphic features of the region. Oktay (1982) and Görür et al. (1984) described the Late Mesozoic and Early Tertiary evolution of the region to the east of the present study area. Özcan et al. (1988) studied the stratigraphy of the area in detail and stated that the Kütahya–Bolkardagi Belt displays different stratigraphic and metamorphic features from the surrounding tectonostratigraphic units. Eren (1993a, 1996a) has investigated the stratigraphic features of the area to the south of Ilgin and Kadinhani towns, west of the present area, and has demonstrated the presence of autochthonous rocks and allochthonous tectonic metamorphic slices; he named these tectonic units the Bozdaglar Massif. Eren (1996a) has also demonstrated that the massif was affected by polyphase deformation. In the present study, the geometry, structural features and structural evolution of the middle part of the Bozdaglar Massif will be discussed. For this purpose, an area of approximately 350 km^2 was mapped and primary and secondary planar/linear structures were observed, and their attitudes were measured.

2. Stratigraphy

The stratigraphy, magmatic activity and petrographic characteristics of the region have been studied in detail by Özcan et al. (1988), Eren (1993b, 1996b), Kurt (1994, 1996), Kurt and Eren (1998) and Göncüoglu and Kozur (1998). For this reason, in this paper the stratigraphy of the region will be outlined only briefly. In the mapped area, the Bozdaglar Massif is made up of Silurian–Lower Permian Sizma and ?Upper Permian–Mesozoic Ardicli Groups (Fig. 2), which are separated from each other by an angular unconformity. Although the rocks of the massif have been subjected to severe polyphase Alpine deformation, the low-grade of the metamorphism allows most of the protoliths and their primary structures to be recognized. The primary structures include bedding, and sedimentary way-up structures, like graded bedding, cross-bedding and ripple marks. For this reason, besides the preserved fossils (Özcan et al., 1988; Eren, 1993a), the primary way-up structures contribute to establishing the stratigraphy of the study area. Cross-bedding and graded-bedding are more common in the Ardicli Group than the Sizma Group.

The Sizma Group is a Hercynian unit of the massif. The oldest rocks in the group form the Bozdag Formation, originally reefal metacarbonates of Silurian–Lower Carboniferous age. The Bozdag Formation is composed of white and light gray marble, dark gray-black bituminous dolomite marble and dolomitic limestone, and passes laterally and vertically into the Devonian–Lower Permian Bagrikurt Formation. The Bagrikurt Formation is made up of an alternation of phyllite, graphite schist, calc-schist, metasandstone, metaconglomerate, and metachert, and includes various shallow-sea and pelagic metacarbonate blocks. The formation has a wild-flysch appearance. These rocks are intruded by the Kadinhani Metamagmatic rocks, which include the Ayyiles metagabbro dykes, the Karadag spilite and, Karatepe metabasaltic andesite. According to Eren (1993a, 1996b) and Eren and Kurt (1998), these magmatic rocks demonstrate the existence of a Paleozoic ocean and a continental magmatic arc, probably older than Late Permian, but certainly older than the Early Triassic.

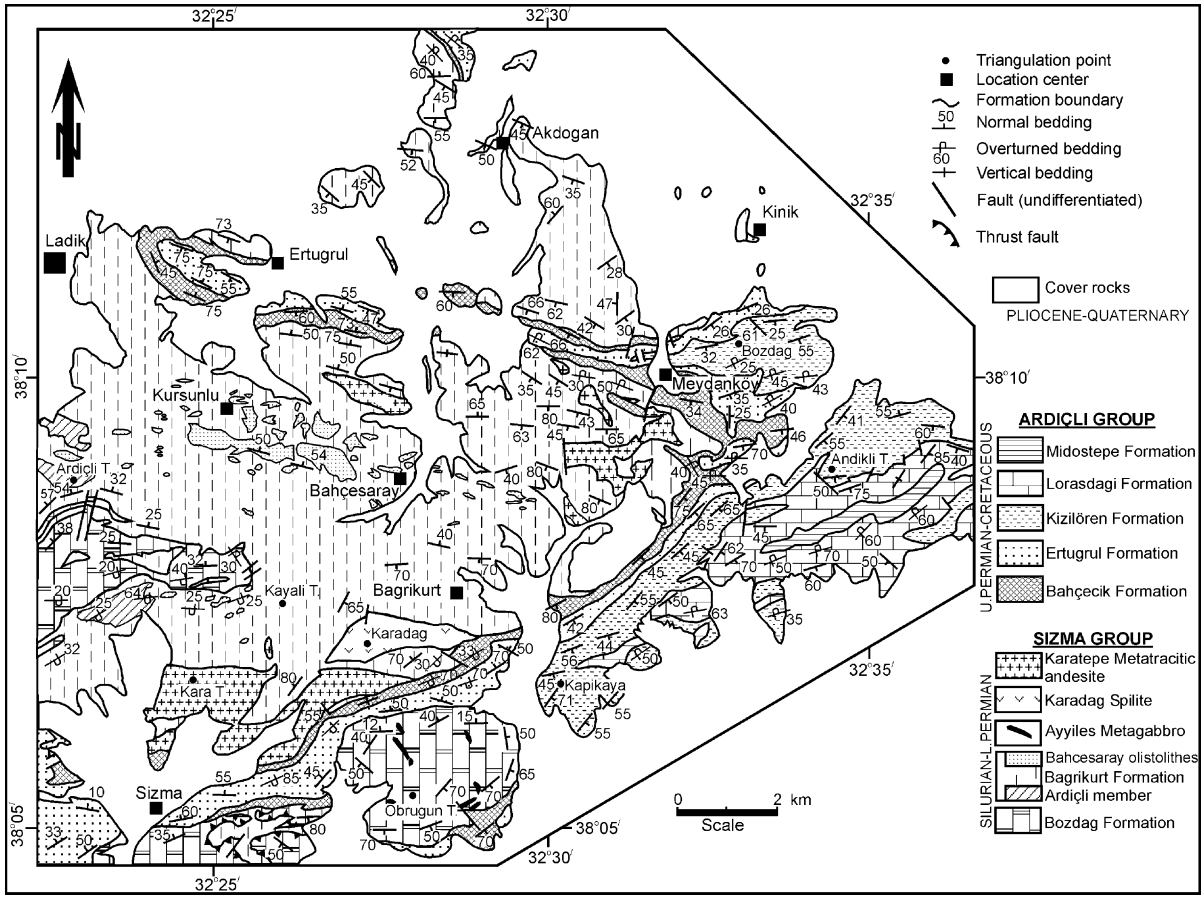

Fig. 2. Geological map of the studied area.

The Sizma Group, which outcrops mainly in the NE part of the area is unconformably overlain by the ?Upper Permian–Mesozoic Ardicli Group. The group is wholly transgressive from base to top and made up of five formations, which interfinger laterally and vertically. The ?Upper Permian–Lower Triassic Bahçecik Formation, lowest unit of the group, is made up of phyllite, metasandstone and metaconglomerate, which originally represented continental clastics. The ?Upper Permian–Triassic Ertugrul Formation consists of an alternation of phyllite, metasandstone, calcschist, and metacarbonate, interfingering with the Bahçecik Formation. The Ertugrul Formation grades conformably upwards into gray and dark-colored dolomites of the Triassic–Lower Jurassic Kiziloren Formation. This unit interfingers with, and is conformably overlain by, a thick sequence of light-colored marble, crystallized limestone, and dolomitic limestone, forming the Upper Triassic–Lower Cretaceous Lorasdagi Formation. In some parts of the formation, lenses and inter-layers of metachert may be observed. The youngest unit of the Ardicli Group is the pelagic Upper Cretaceous Midostepe Formation. The formation includes well-bedded metachert, metacarbonate, phyllite and metasandstone. In the study area, Pliocene–Quaternary continental rocks rest unconformably on all the older units and form the unmetamorphosed cover rocks of the massif.

3. Structural geology

The stratigraphic and lithologic features of the rocks, with their metamorphic and magmatic features indicate that both Hercynian and Alpine orogenic activity affected this region (Özcan et al., 1988; Eren, 1993a, 1996a; Kurt, 1994), but severe polyphase Alpine deformation and metamorphism has obliterated the pre-Alpine structures of the Sizma Group. The only Hercynian structures recognized are pre-Alpine overthrusts, which separate rock units of the Bozdag and Bagrikurt Formations (Eren, 1996c). This paper describes only the Alpine structures in the area.

Field observation, map-scale and microscopic studies show that the Paleozoic and the Mesozoic rocks of the mapped area are metamorphosed and have been subjected to at least four deformational events; these are designated as D_1, D_2, D_3 and D_4 (Figs. 2–5). Due to polyphase deformation, all the rock units are strongly folded and display good examples of refolded folds (F_1, F_2, F_3, F_4), with both penetrative (S_1) and non-penetrative cleavage (S_2, S_3, S_4), and lineations (L_1, L_2, L_3, L_4) related to crustal shortening.

The dimension of the folds ranges from mega- to microscopic scale. The main map-scale structures are the Akdogan Anticline and the Ertugrul Syncline, which developed during F_1-folding (Figs. 2, 3 and 6). The Akdogan Anticline

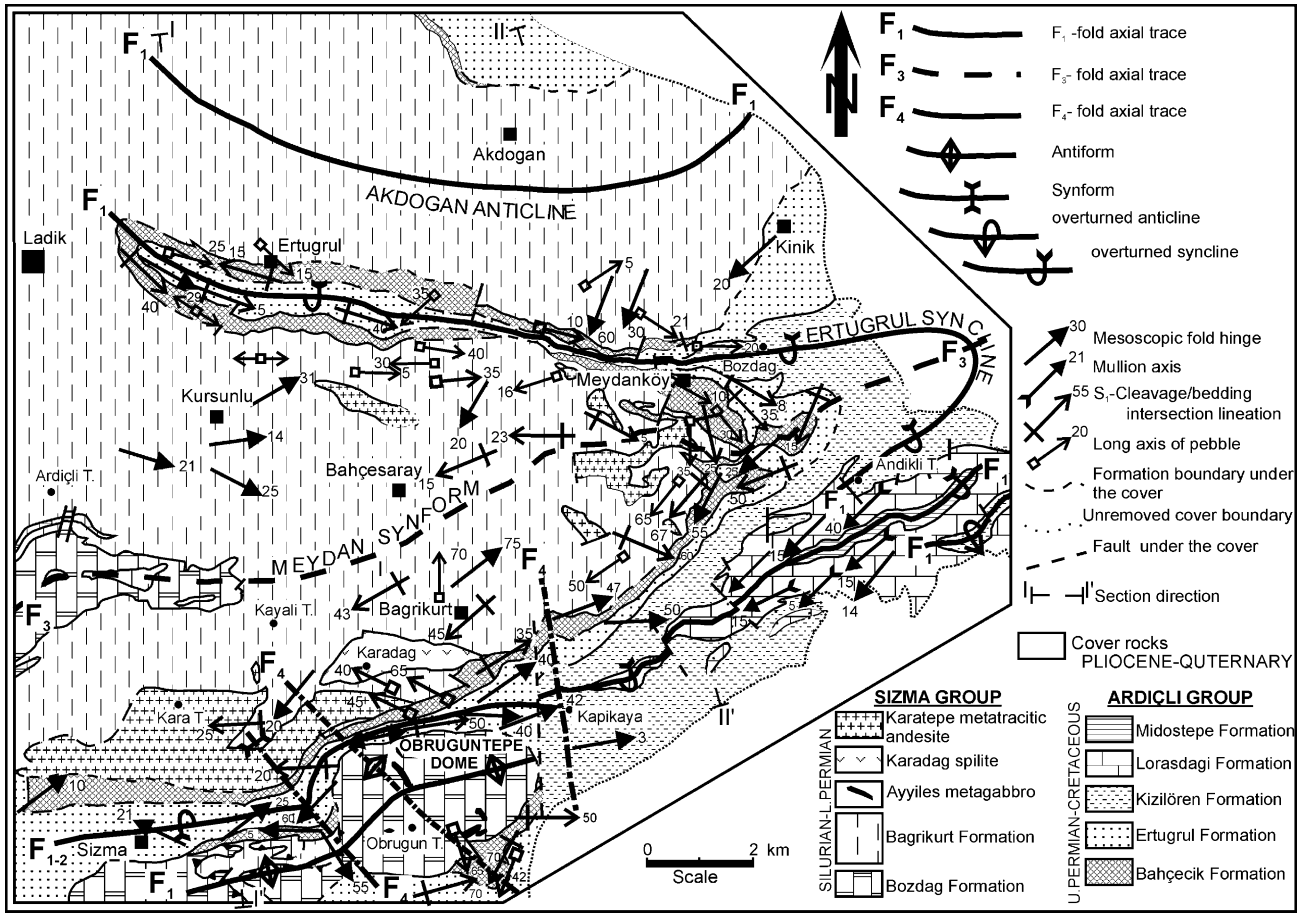

Fig. 3. Structural map of the studied area, showing major structural features and mesoscopic fold axes (where possible, the cover rocks have been removed to show the main structures).

crops out in the northern part of the study area but is extensively covered by the young rocks. The Ertugrul Syncline can be traced over about 34 km in the study area, with rocks of the Ardicli Group outcropping in its core. Due to subsequent folding, the fold hinges and axial surfaces of the Ertugrul Syncline show a wide variation in orientation. For structural analysis, the mapped area has been subdivided into the six domains (Fig. 4) for which all the structural elements were plotted (Fig. 7). The results are summarized in Table 1. The Ertugrul Syncline has a mean fold hinge plunge of 12°/108° and between Ladik and Ertugrul villages (Domain I) has a nearly vertical NW–SE trending axial surface. From Ladik to Meydanköy village (Domain II), the mean fold hinge orientation of the Ertugrul Syncline is 4°/290° with a 101°/44° SW oriented axial surface. In this domain, the minor F_1-folds verge to the northeast and have an isoclinal geometry. To the east of Meydanköy village, the syncline is affected by F_3-folding, and the Ertugrul Syncline swings to a NE–SW trend between the Andikli and Kapikaya Hills (Domain III). In this domain, the mean plunge of the hinge of the syncline is 15°/225°. Associated minor folds are tight to isoclinal in geometry and are overturned to the northwest with a mean axial surface orientation of 070°/52° SE. In this domain, all the formations of the Ardicli Group crop out in the core of the Ertugrul Syncline (Figs. 2, 3 and 6). To the west of Kapikaya Hill, the hinge of the syncline curves sharply, and the dips of the axial surfaces and the plunges of the fold hinges of F_1-folds change to the opposite direction (Domain IV). Thus, between the Karadag and southern part of the Bagrikurt village, the Ertugrul Syncline has a SSE vergence with a mean axial surface orientation of 080°/70° NW; the mean orientation of the fold hinge is 33°/063°. Due to F_4-folding, the trace of the Ertugrul Syncline curves sharply and continues to the west of the Sizma village (Domain V). In this domain, the Ertugrul Syncline has a southerly vergence, an axial surface orientation of 067°/51° NW, and a mean fold hinge orientation of 14°/254° (Figs. 3 and 7).

The second phase of deformation did not produce map-scale folds so that the other most striking map-scale structure in the area is the D_3-Meydan Synform. The Meydan Synform displays a Type-2 (Ramsay, 1967) fold interference pattern on the map scale (Fig. 3). The Meydan Synform can be traced over 18 km in an east–west direction and has a width of approximately 10.5 km. The Bozdag Formation, which is the oldest formation in the study area, crops out in the core of the Meydan Synform and the other units of the Sizma Group and the Ardicli Group occurs on its limbs. Due

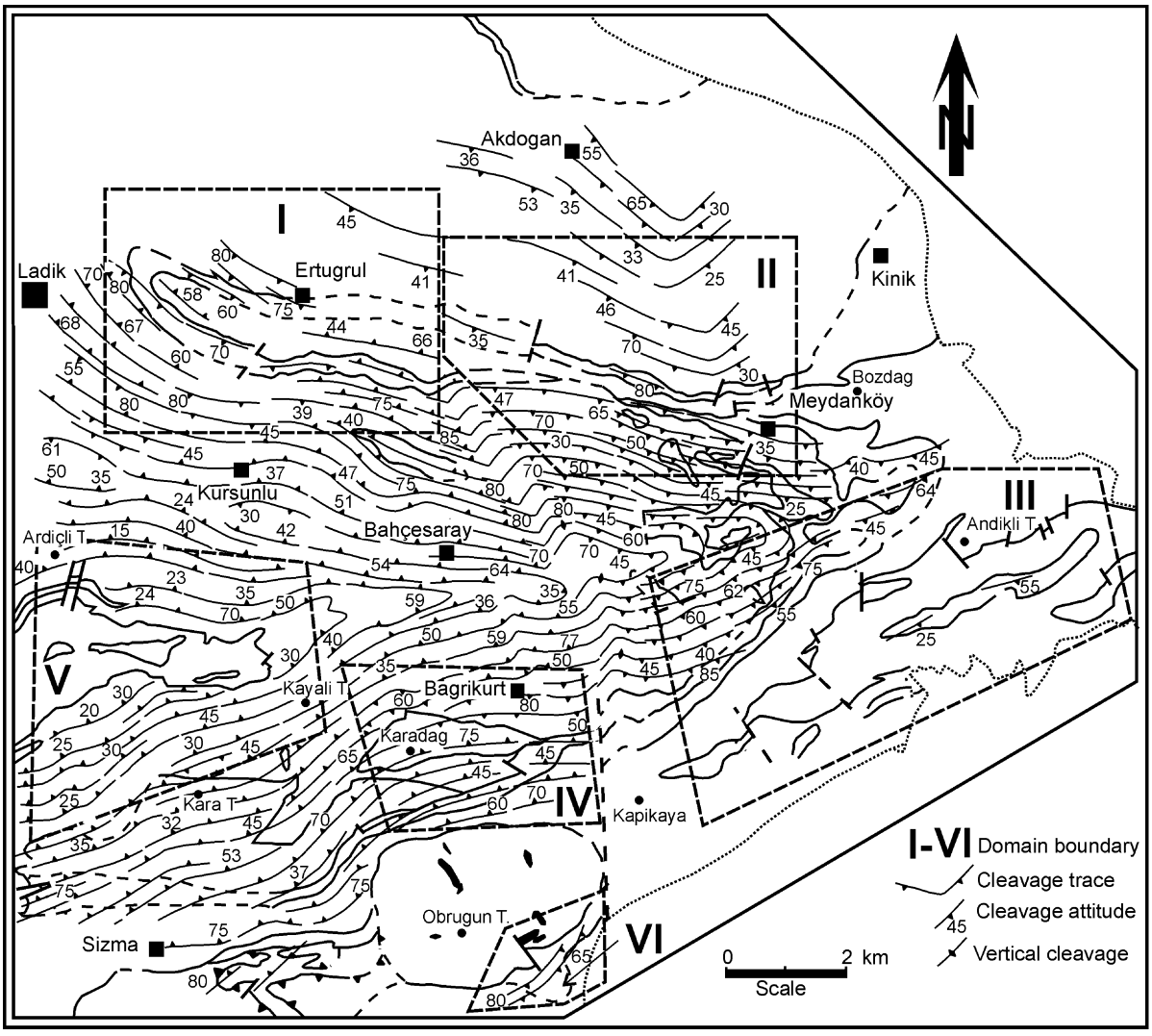

Fig. 4. Structural map of the studied area showing domain boundaries and traces of D_1-phase cleavage surfaces (other symbols are the same as Fig. 2).

to this folding, F_1- and F_2-mesoscopic fold axes, bedding and cleavage intersection lineations (S_0/S_1), and the long axes of pebbles deformed in D_1 show marked dispersion near Meydanköy village. According to the orientation of the bedding planes measured around Meydanköy village, the mean orientation of the fold hinge of the Meydan Synform is 44°/213° (Fig. 7). S_1-surfaces, developed axial planar to the F_1-folds, are also deformed and folded as a result of F_3-folding, but are transposed parallel to S_3 near the F_3-fold hinge to the southeast of Meydanköy village (Fig. 4). The other map-scale folds are of kink-fold type and belong to the F_4-folding event. To the northwest of the Obrugun Hill the Ertugrul Syncline was sharply refolded between the two nearly parallel NW–SE trending F_4-axial surfaces (Figs. 3 and 4). Furthermore, the change of the vergence of the Ertugrul Syncline around the Kapikaya Hill, from NW (in domain III) to SE (in domain IV), was most probably related to the formation of the F_4-folds. Between this location and 2 km SE of Ertugrul village, approximately in a NW trending zone, the dip of the S_1-cleavage surfaces changes sharply from a southerly to a northerly direction. Although this zone is mostly overlain by younger cover rocks (Fig. 2), it can be interpreted as a kink-zone as resulting from F_4-folding. On the other hand, the superposition of the F_4-folds over the F_1-folds generated Type-1 dome and basin structures. The Obrugun Hill dome is an example of one of these structures (Fig. 3). Due to these polyphase deformation events, a wide variety of mesoscopic and microscopic interference structures were formed.

3.1. D_1-structures

The F_1-minor folds have interlimb angles of 60–0°, and are generally tight to isoclinal, asymmetric, overturned folds; with an axial planar S_1-cleavage (Fig. 8A). The bedding in the Bagrikurt and Bahçecik Formations, in which metapelites are the most common rock type, is generally transposed by F_1-folds and shows intrafolial fold

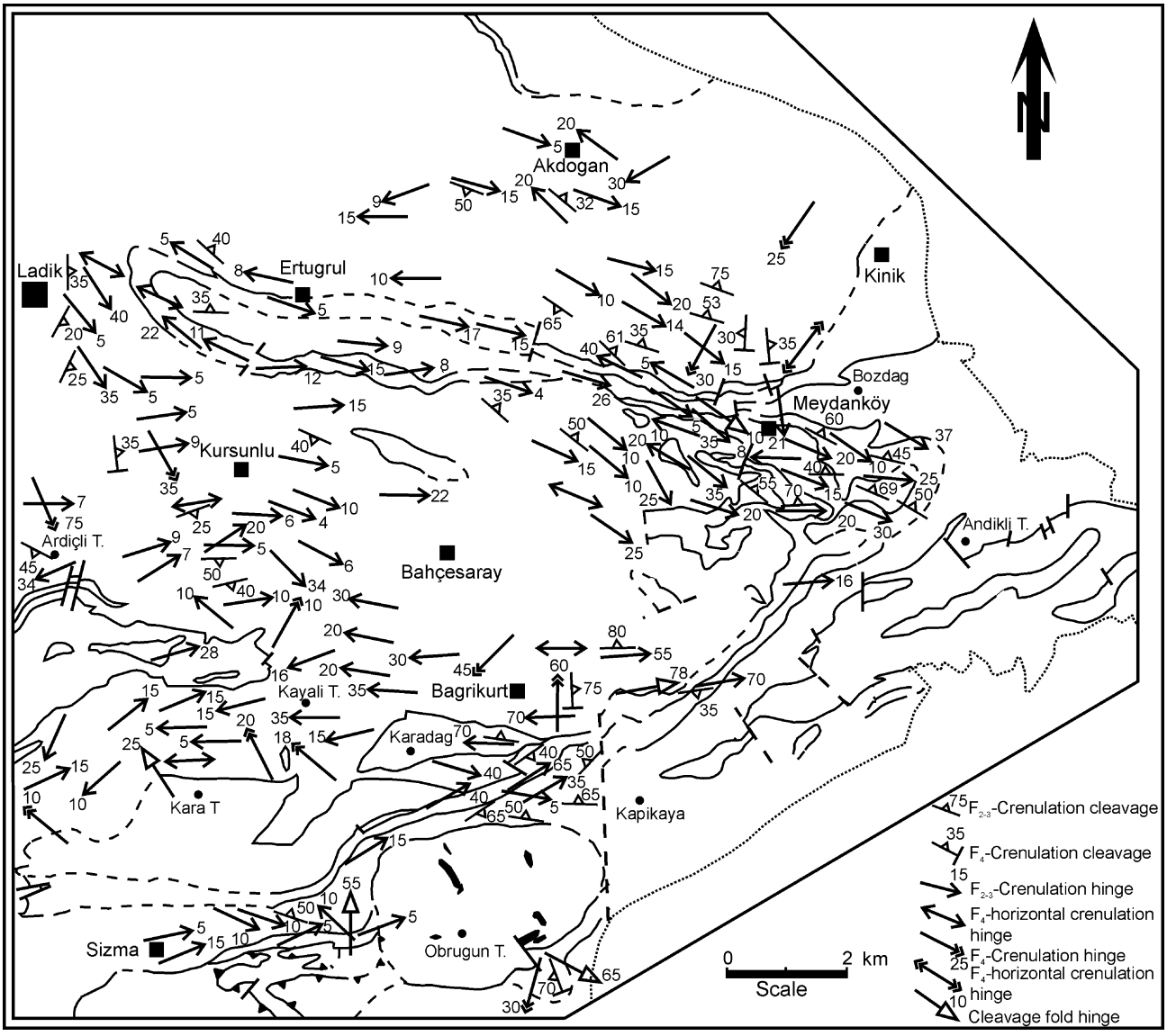

Fig. 5. Structural map of the studied area showing $D_{2,3}$- and D_4-phase mesoscopic planar and linear elements (other symbols are the same as Fig. 2).

geometry. However, F_1-folds can be observed widely in the Ertugrul Formation, which is composed of an alternation of well-bedded competent and incompetent rocks. The wavelengths of the F_1-folds range from 1 cm to 50 m. The F_1-folds in the competent rocks generally have class-1C geometry (Ramsay, 1967) and the overturned limb is generally thinned (Fig. 8B). Sigmoidal and en echelon tensional veins can be observed in the limbs of the folds. Mesoscopic fold hinges show a wide variation in attitude, due to polyphase folding (Figs. 3 and 7).

The other most prominent structure is a penetrative S_1-cleavage, developed on a regional scale. S_1-planes cut continuously through the appropriate rocks of the the Sizma Group, the Kadinhani Metamagmatics, and the Ardicli Group. S_1 is axial planar to F_1-folds and shows convergent and divergent cleavage fans (Fig. 8A). S_1-cleavage planes, which are present in both recumbent isoclinal folds of the competent rocks and in the incompetent rocks, are truly parallel to the axial plane of the F_1-folds (Fig. 8C). For this reason, in the limbs of the large isoclinal folds, S_1-cleavage planes are nearly parallel to the bedding. Where there are lithological contrasts, cleavage refraction can be observed. In this situation, S_1-cleavage planes have a different orientation and a different spacing (Fig. 8A and D). In slate and phyllite, S_1 can be termed a slaty cleavage (continuous cleavage; Powell, 1979), whereas their continuation in the competent rocks (metasandstones and marbles) are spaced cleavages. In marble and quartzite, both cleavage and bedding surfaces are generally stylolitic and are enriched in phyllosilicates and dark minerals.

An anastomosing cleavage can be observed in the originally matrix-supported metaconglomerates of the Bagrikurt and Bahçecik Formations. The pebbles of these metaconglomerates are strongly flattened parallel to the cleavage

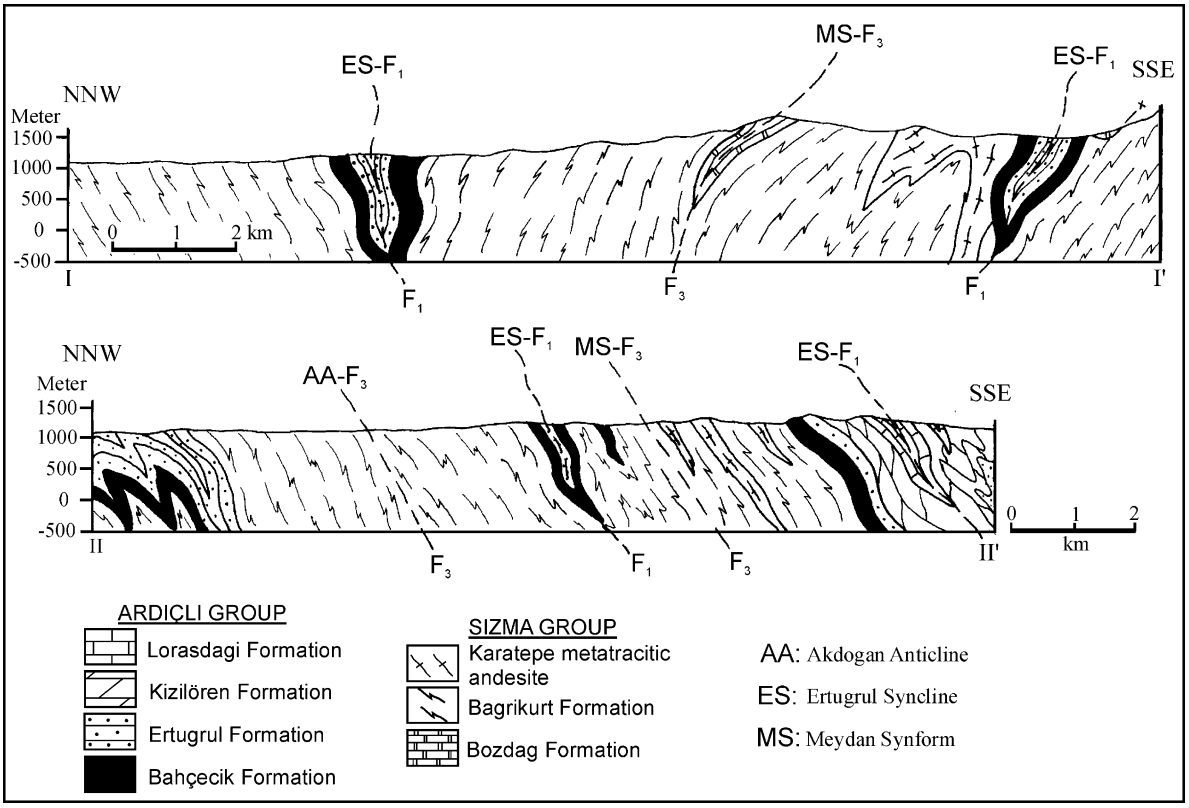

Fig. 6. Structural cross-sections of the studied area. Lines of sections shown in Fig. 3.

planes (Fig. 8E). On the other hand, cleavage in calcite-, or FeO-cemented metaconglomerate is not obvious, and the pebbles are less deformed; stylolites are common at the contacts of the pebbles (Fig. 8F). In the metasandstones, the clasts are flattened parallel to the cleavage planes, and pressure shadow zones were developed around them. In pressure shadow zones quartz, muscovite/sericite, albite, chlorite, graphite, calcite and stilpnomelane mineral growth has occurred. In the matrix of the metasandstones, slates and phyllites, preferred orientation and new growth of the same minerals, together with chloritoid, define S_1.

On the microscopic scale S_1 is generally of continuous cleavage type. Quartz crystals show undulatory extinction. Deformation twins and kinking can be observed in calcite and feldspar. Thick quartz veins (1–25 cm) occur parallel to S_1-planes, especially in metapelites In addition, fibrous quartz veins perpendicular to the cleavage are observed in the rocks of the massif, developed both normal and parallel to minor F_1-fold hinges. This indicates that additional extension occurred parallel to the fold hinges during the D_1-phase of deformation. These quartz veins are deformed and folded by subsequent fold phases. In metaigneous rocks the preferred orientations of amphibole, muscovite/sericite, chlorite and feldspar minerals form S_1-planes and pass continuously into the surrounding rocks. Glaucophane crystals, which are developed around the rims of pyroxene minerals, are also oriented parallel to the cleavage surfaces. From these observations, it is deduced that, depending on rock type, flattening, plastic deformation, the rotation of grains, metamorphic mineral growth, and pressure solution are the main cleavage forming mechanisms.

The most common lineation is S_0/S_1-intersection lineation. These lineations show similar orientations to the F_1-fold hinges (Figs. 3 and 7). Another prominent lineation is formed by the long axes of pebbles. On the limbs of the folds, the long axes of pebbles are generally perpendicular to the fold hinge, whereas in the hinge zones they are nearly parallel to the fold hinges (Figs. 3 and 7). Pebbles are flattened and elongated in S_1 with their longest axes (X) and intermediate axes (Y) in S_1, and their shortest axes (Z) normal to S_1. The shape of deformed pebbles is generally oblate or pancake-shaped, but at some localities the pebbles have cigar-like form. The amount of strain depends on pebble composition, matrix type and position in the folds. The pebbles in the metaconglomerates are quartzite, milky quartz, metasandstone, dolomite, marble, metachert and phyllite. Metachert and phyllite clasts in the Bagrikurt Formation are intraformational clasts, in origin.

About 1500 deformed pebbles were measured in the field, at 40 localities. The details will be given in another paper, but preliminary results are summarized here. In the strain calculation given below, the initial shape of the pebbles is assumed to have been a sphere and volume loss has been neglected. In the deformed pebbles, the R_{XY} ranges from 1.1 to 3.4, R_{XZ} ranges from 2 to 13, and R_{YZ} ranges from 1.4 to 4.3. Most of the pebbles lie in the field of the apparent

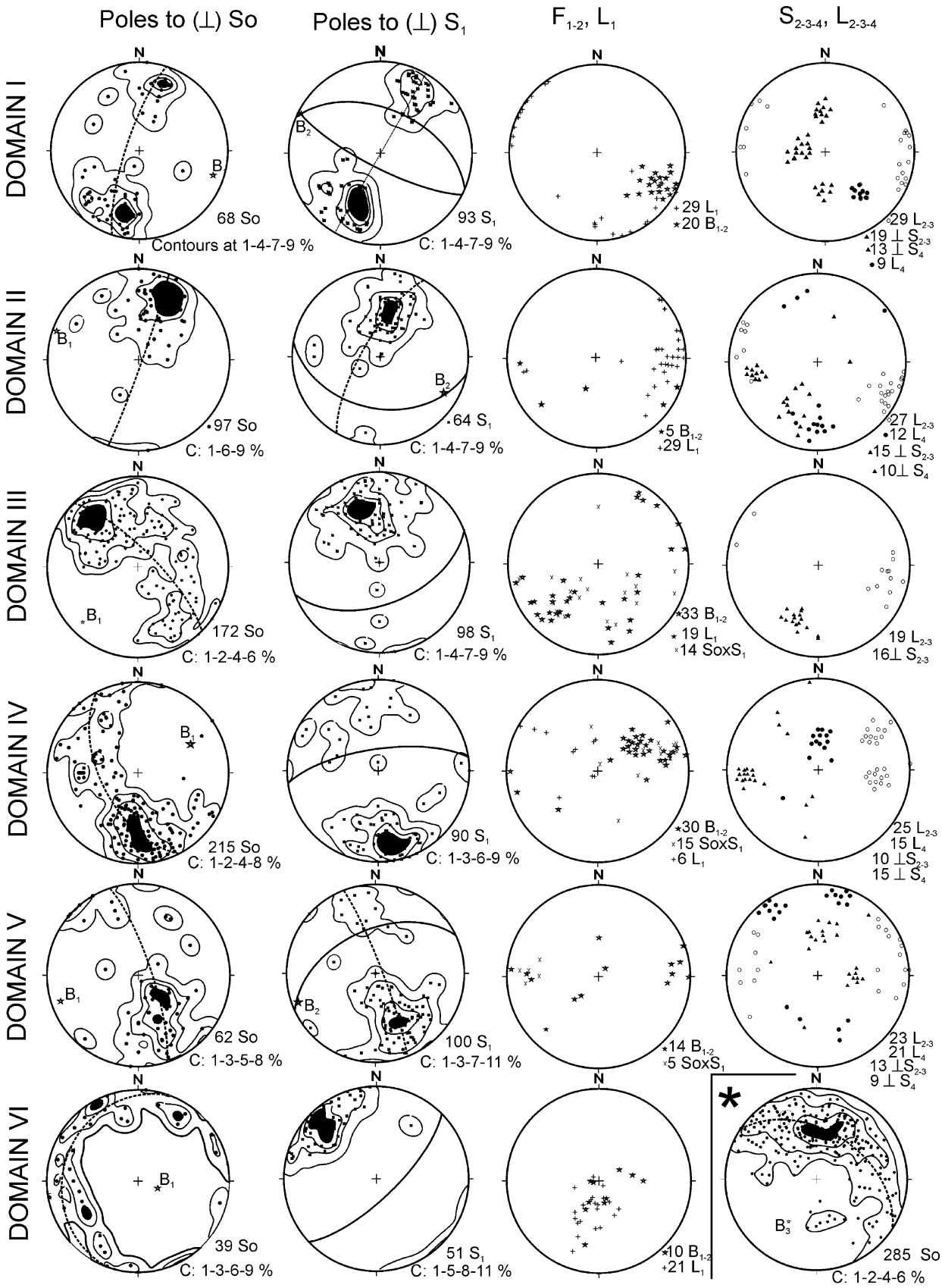

Fig. 7. Lower-hemisphere projections of the mesoscopic data from the domains of the study area (●: pole to bedding; ■: pole to cleavage; *: fold hinge, ×: S_0/S_1-intersection lineation; +: long axis of pebble; ○: L_{2-3}-crenulation hinge; ·: L_4-crenulation hinge; ▲:pole to crenulation cleavage). Other explanations in the text and Table 1.

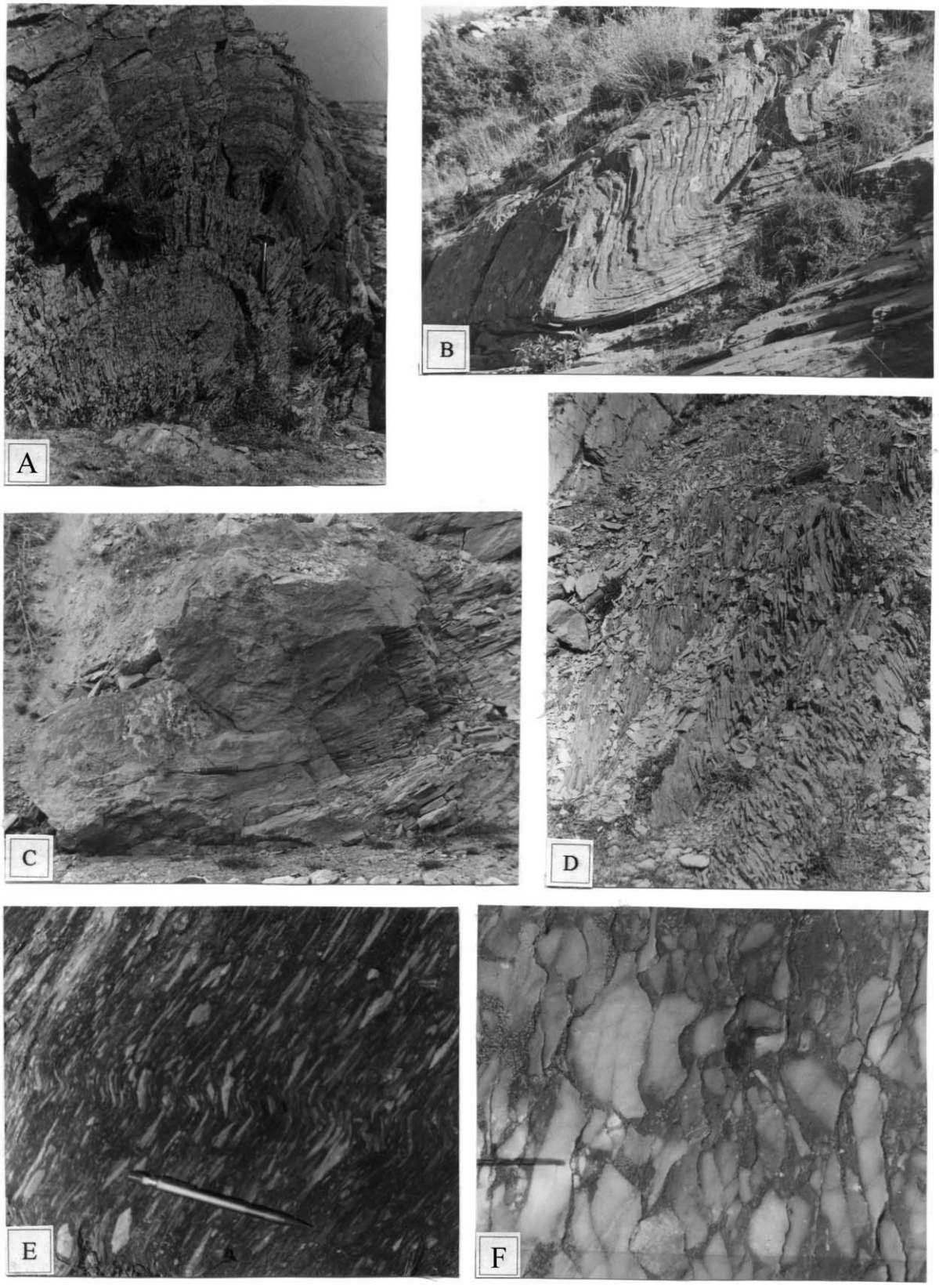

Fig. 8. D_1-structurres: (A) Fanning S_1-axial planar cleavage in folded metacarbonates and calcschists (?U. Permian–Triassic Ertugrul Formation). (B) Overturned F_1-folds in the metacarbonates of the Ertugrul Formation. Note the thinning of the long limbs. (C) S_1-cleavage in folded phyllite and sandstone, Ertugrul Formation. (D) S_1-cleavage refraction in phyllite, calcschist and marble, Ertugrul Formation. (E) Metaconglomerate strongly deformed and cleaved during the D_1-phase, ?U. Permian–L. Triassic Bahçecik Formation. The flattened pebbles were linked later by the D_3-phase of folding. (F) Metaconglomerate deformed predominantly by pressure solution during the D_1-phase, Bahçecik Formation.

flattening, but a few lie in the field of apparent constriction of Flinn (1962) graph. For flattened pebbles k values are between 0.042 and 0.7, and for constricted pebbles between 1.1 and 5.36. The estimated extension (e) parallel to the X-direction changes from 40 to 185%. But more extension (up to 265%) occurs in phyllite (originally mud) pebbles. Mullion structures can also be observed in the rocks. Especially, in the Lorasdagi and Midostepe formations, thin metachert beds are deformed as long cylinders and form the main linear structure in these rocks. The long axes of the mullion structures are parallel to the minor F_1-folds (Fig. 3). On the other hand, in well-bedded and well-cleaved formations, the intersection of cleavage and bedding separates the rock into long, angular, prismatic fragments (pencil cleavage).

3.2. D_2-structures

The D_2-deformation event may be recognized where it refolds bedding planes and S_1-cleavages. F_2-folds are developed coaxially to F_1-folds, and the superposition of F_1- and F_2-folds creates Type-3 refolded folds. (Fig. 9A). Type-3 refolded folds are generally observed on the outcrop scale. F_2-folds are close to tight, with a wavelength ranging from 1 cm to 5 m, and show cylindrical to zigzag shapes in profile. These folds mostly show axial planar crenulation cleavages (S_2) (Fig. 9B), with crenulation axes parallel to F_2-fold hinges. The S_2-cleavage planes also show fanning around the fold and their spacing varies with rock type, so that both zonal- and discrete-type crenulation cleavages occur, even in the same sample. The shape of S_2-surfaces, perpendicular to the crenulation axis, changes from stylolitic to regularly oriented. Where the microfolds are open, the crenulations form en echelon, short, dark-colored, separate zones across the limbs of the microfolds. As tightness of the fold increases, the width and length of the crenulations also increases. Cleavage zones are mostly depleted of quartz and light-colored minerals. The traces of the muscovite and chlorite in the S_1-cleavage zones pass continuously through S_2-cleavage zones, only changing in orientation. However, flattened quartz grains or quartz porphyroblasts, which occur with chlorite and mica minerals in the S_1-cleavage planes, terminate abruptly at the S_2-boundary. This shows that quartz and other light-colored minerals, which occur between mica and chlorite in the S_1-surfaces, have been dissolved in the S_2-zones. Despite the presence of chloritoid nearly parallel to S_2-zones in the S_1-fabric (outside the S_2-fabric), no mineral growth of chloritoid has been observed. Some chloritoid porphyroblasts are oriented parallel to the S_1-fabrics, but some chloritoid crystals overgrow the S_1-fabric, and the S_1-fabric terminates abruptly at the boundary of these chloritoid crystals. In other words, chloritoid formation is both syn- and post-tectonic with respect to D_1. This suggests that metamorphism with chloritoid growth continued throughout the D_2-event.

3.3. D_3-structures

The superposition of F_3-folds over F_1-folds gave rise to the Meydan Synform, which is the main structure in the studied area. On the other hand, the D_3-event formed S_3-crenulation cleavages, L_3-lineations, and monoclinal and conjugate kink folds. The shape and microscopic features of the S_3-crenulation cleavages and lineations are similar to those of the D_2-structures. Even if there are slight differences in the orientation of S_2 and S_3, it is not always possible to differentiate one from the other. However, when two cleavages develop in the same outcrop, it is possible to differentiate them, due to the overprinting. The width of F_3-kink folds ranges from 1 mm to 1 m in outcrop scale. They are widely developed in phyllite, calcschist, cleaved metasandstone and metaconglomerate (Fig. 8E). Although kink folds are developed throughout the studied area, they are most commonly developed in the Bahçecik and Ertugrul formations from the west of Meydanköy village to the north of Sizma (on the southern limb of the Meydan Synform), parallel to the outcrop trends of these formations. Large kink folds (ranging from 10 cm to 1 m width) generally occur as monoclinal sets (Fig. 9D), and are lens-shaped. The small-scale kink folds generally occur as conjugate sets, although the two sets are not always equally developed. L_3-crenulation lineations are parallel to one set of the conjugate kink fold hinges (Fig. 9C). The dominant conjugate kink bands are contractional (reverse) type and deform both S_1 and S_2 (Fig. 9E).

3.4. D_4-structures

D_4-structures vary from microscopic to macroscopic in scale. D_4 resulted in microscopic S_4-crenulation cleavages and mesoscopic F_4-conjugate kink folds, displaying the same features as F_3-kink folds both in size and shape. The hinges of D_4-kink folds were developed approximately at right angles to the F_3-kink folds, and deform L_3-lineations (Fig. 9F). Crenulation axes trend NE–SW and NW–SE, with variable plunge. S_4-crenulation cleavages strike generally from N to S and dip W or E (Figs. 5 and 7). The L_4-crenulation hinges are generally parallel to one set of the F_4-kink fold hinges, indicating a close relationship between crenulation cleavage and kink band development. The S_4-crenulation cleavage and lineation are similar to the other crenulations, but generally occur on a finer scale. Microscopic observations have not shown any new metamorphic mineral growth parallel to the crenulation cleavage.

4. Discussion

The deformation history of an S_0-bedding plane through the four deformation phases is shown diagrammatically in Fig. 10. During D_1, bedding planes (S_0) in all stratigraphic units were overturned towards the south and isoclinally folded in the major E–W Ertugrul Syncline (Figs. 6 and

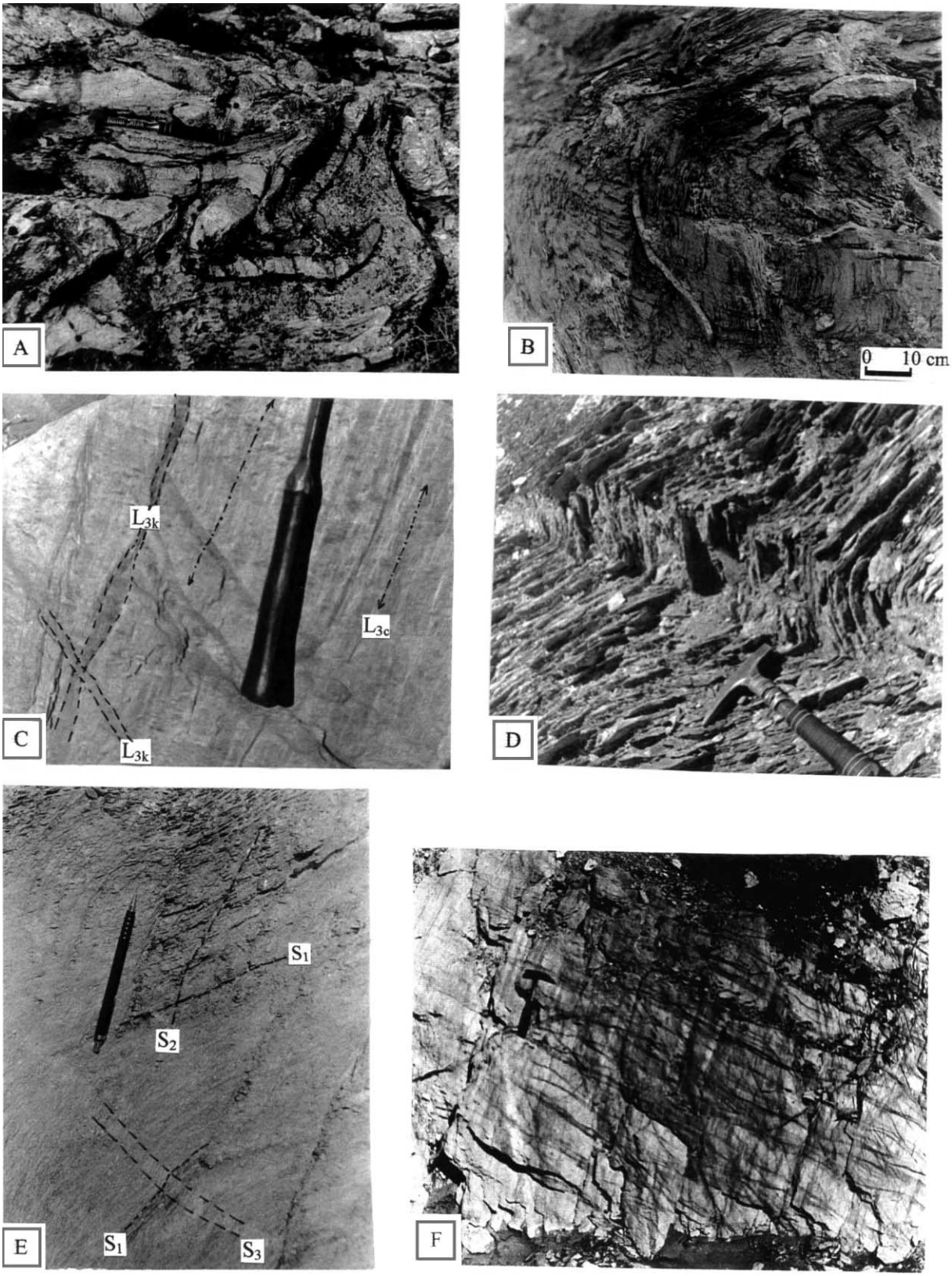

Fig. 9. D_2–D_4 structures. (A) Type-3 refolded folds which developed by the superposition of F_2-folds over F_1-folds in metachert and metacarbonate of the Upper Cretaceous Midostepe Formation. (B) Folded quartz vein and S_1-cleavage with axial planar crenulation cleavage (S_2) in phyllites of Bahçecik Formation. Note the fanning of the crenulation cleavage planes. (C) D_3-phase conjugate kink folds with crossing axes (L_{3k}) and crenulation lineations (L_{3c}) on the S_1-cleavage plane, phyllite, Bahçecik Formation. (D) Third phase (D_3) monoclinal kink band developed in strongly cleaved slates and metasandstones of the Bahçecik Formation. (E) First phase slaty cleavage (S_1) and second phase crenulation clevage (S_2) deformed by the third phase kink band (S_3). (F) D_3- and D_4-phases related conjugate kink bands (L_3, L_4) developed on the S_1-cleavage planes (metasandstone, Bahçecik Formation).

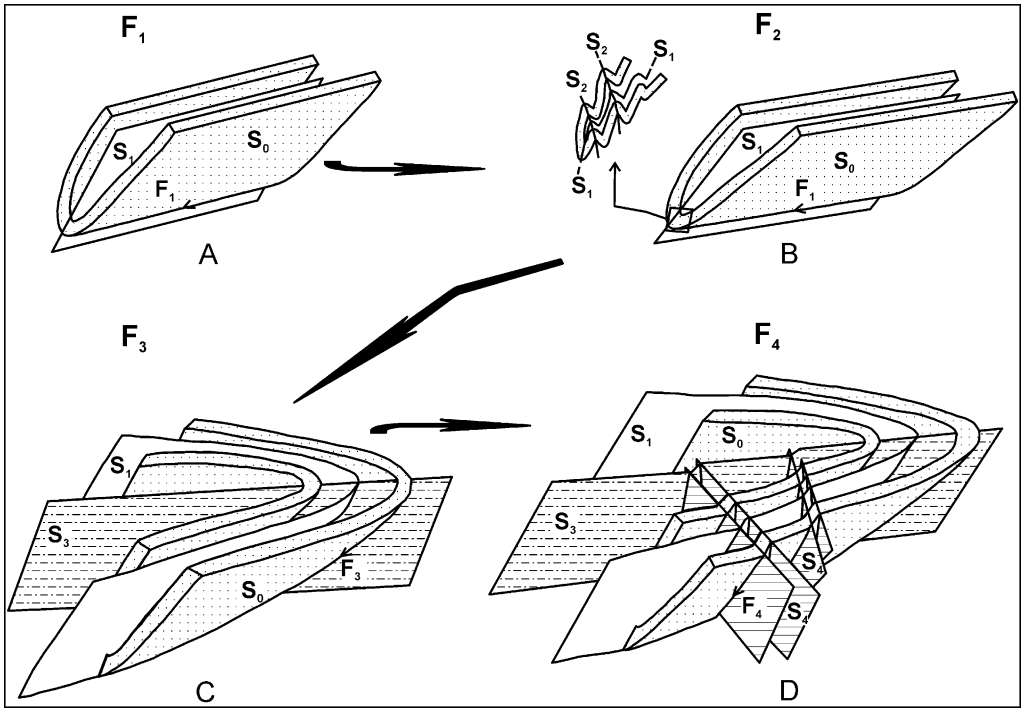

Fig. 10. Kinematic evolution (schematic) of the Meydan Synform.

10A). The presence of a pervasively and regionally developed S_1-cleavage surface, axial planar to F_1-folds, and strongly deformed conglomerates indicates that the D_1-deformation occurred in a N–S ductile shortening regime. The Paleozoic and Mesozoic rocks of the massif were subjected to high pressure/low temperature metamorphism (Kaaden, 1966; Bayiç, 1968; Özcan et al., 1988; Eren 1993a; Kurt 1994). The pressure–temperature conditions of metamorphism have been calculated as 6–7 kbar and 350–400°C for blueschist facies metamorphism (Kurt, 1996), suggesting a depth of burial to 25 km. The age of the metamorphism has not yet been determined. However, geological investigations to the north of the Menderes Massif and the Afyon–Bolkardagi Belt suggest that blueschist metamorphism was completed before the late Cretaceous (Okay, 1986). But, the youngest metamorphosed rocks in the study area are of Upper Cretaceous in age, and in the Afyon–Kütahya region, the metamorphic units are covered unconformably by post-orogenic Upper Paleocene–Eocene sedimentary rocks (Özcan et al., 1990). For this reason, the metamorphism is considered to have occurred between the Late Cretaceous and Middle Paleocene to the north of Konya. The parallel orientation of the main metamorphic minerals and the S_1-cleavage demonstrates that the peak of metamorphism occurred during the D_1-deformation event.

The metamorphic rocks are mainly of continental origin in this region, suggesting that metamorphism was the result of the obduction of an ophiolite body onto the continental margin of the Menderes–Taurus Block (Sengör and Yilmaz, 1981), or to the subduction of the continental margin of the Menderes–Taurus Block under the oceanic lithosphere in the intra-oceanic subduction zone (Okay, 1984) due to closing of the Inner Tauride Ocean. Continuing N–S crustal shortening resulted in the coaxial folding of bedding, and of S_1-planes related to the F_1-folds, during the D_2-deformation phase (Fig. 10B). D_2 may have resulted from progressive shortening during a single phase of deformation. Microscopic studies indicate that mineral growth under metamorphic conditions continued during the D_2-phase. The absence of any metamorphic minerals, except chloritoid porphyroblasts, parallel to S_2 shows that the high-*P*/low-*T* conditions ended with the D_1- event, and the metamorphism changing from blueschist to the greenschist facies conditions during D_2. Comparison of D_1- and D_2-structures confirms that D_1-deformation phase was more intense than D_2-deformation phase.

Superposition of F_3-folds on the major Ertugrul Syncline, and its associated minor asymmetrical folds, created the map-scale Meydan Synform, also suggests N–S shortening (Fig. 10C). This deformation phase also created monoclinal and conjugate kink folds and the S_3-crenulation cleavage. The development of widespread kink bands indicates that deformation occurred in the ductile–brittle transition. Further E–W shortening during the D_4-phase, has generated monoclinal/conjugate kink folds on various scales (Fig. 10D) and an S_4-crenulation cleavage, similar to those of the D_3-phase. Since the same structures have developed during the D_3- and D_4-phases, the same deformation conditions must also have prevailed during the D_4-phase. F_4-fold hinges are developed nearly orthogonal to F_3-folds indicating a marked change in the shortening direction. The absence of any new mineral growth parallel to the S_3- and

S_4-planes indicates that during these phases the temperature had fallen below the level of metamorphism.

5. Conclusions

The northern margin of the Menderes–Taurus Block to the north of Konya has undergone a polyphase and complex history of tectonic events (D_1-D_4) due to closing of the Inner Tauride Ocean. The first phase of deformation (D_1) probably took place in a subduction zone environment at between 20 and 25 km depth (Kurt, 1996) and was coeval with Late Cretaceous–Middle Paleocene high-*P*/low-*T* metamorphism. The D_1-deformation phase generated the major upright isoclinal Ertugrul Syncline, overturned, tight to isoclinal minor folds, and a regionally developed, penetrative S_1-cleavage. The second deformation phase (D_2), coaxial with the D_1-phase, produced only tight minor (F_2-folds) folds and formed Type-3 refolded folds on the outcrop scale, with an axial planar S_2-crenulation cleavage. The third phase of deformation (D_3) overprinted earlier structures and produced the major upright Meydan Synform and developed map scale Type-2 refolded folds. D_3-phase structures are a S_3-crenulation cleavage, monoclinal and conjugate kink folds. The last phase of deformation (D_4) created S_4-crenulation cleavage and another system of conjugate kink folds that range from outcrop to map-scale. The D_1- and D_3-deformation phases are represented by major folding phases in the study area. Finally, microscopic examination shows that the D_3- and D_4-phases were post-metamorphic deformations.

Acknowledgements

The author is indebted to Prof. J.F. Dewey and Dr J.E. Treagus for constructive reviews of an earlier version of the paper, which improved the presentation of the work. Dr A.J. Barber has improved the English.

References

Bayiç, A., 1968. About the Sizma–Konya metaporphyries. Mineral Research and Exploration Bulletin 70, 214–228 (in Turkish).

Eren, Y., 1993. The geology of the Eldefl–Derbent–Tepeköy–Sögütözü (Konya) region. Unpublished PhD thesis, Selçuk University, Konya, 224 pp. (in Turkish, with English abstract).

Eren, Y., 1993b. Stratigraphy of autochthonous and cover units of the Bozdaglar Massif NW Konya. Geological Bulletin of Turkey 36, 7–23 (in Turkish, with English abstract).

Eren, Y., 1996a. Structural features of the Bozdaglar massif to the south of Ilgin and Sarayönü (Konya). Geological Bulletin of Turkey 39 (2), 49–64.

Eren, Y., 1996. Stratigraphy and geological evolution of the Bozdaglar Massif in the south of Ilgin and Sarayönü (Konya). In: Korkmaz, S., Akçay, M., (Eds.), Karadeniz Technical University Department of Geology 30th Year Symposium, Proceedings, II: 694–707 (in Turkish, with English abstract).

Eren, Y., 1996c. Pre-Alpine overthrusts in the north of Sille-Tatköy (Bozdaglar Massif-Konya). Bulletin of the Geological Congress of Turkey 11, 163–169 (in Turkish, with English abstract).

Eren, Y., Kurt, H., 1998. The geological evolution of northern margin of the central part of Menderes–Tauride block. METU, Third International Turkish Geology Symposium, Ankara, p. 289 (Abstracts).

Flinn, D., 1962. On folding during three-dimensional progressive deformation. Quarterly Journal of the Geological Society of London 118, 385–433.

Göger, E., Kiral, K., 1969. Geology of the Kizilören region. Mineral Research and Exploration Report No.: 5204 (in Turkish).

Göncüoglu, M.C., Kozur, H., 1998. Facial development and thermal alteration of Silurian rocks in Turkey. Proceedings of the Sixth International Graptolite Conference and 1998 Field Meeting of the IUGS Sub-Commission on Silurian Stratigraphy, Temas Geologico-Mineros-ITGE, 23, pp. 87–90.

Görür, N., Oktay, F.Y., Seymen, F.Y., Sengör, A.M.C., 1984. Paleotectonic evolution of the Tuzgölü basin complex, Central Turkey: sedimentary record of a Neo-Tethyan closure. In: Robertson, A.H.F., Dixon, J.E. (Eds.), The Geological Evolution of the Eastern Mediterranean. Geological Society of London Special Publication 17, 467–482.

Kaaden, W.G., 1966. The significance and distribution of glaucophane rocks in Turkey. Mineral Research and Exploration Bulletin 67, 36–67.

Ketin, I., 1966. Tectonic units of Anatolian Asia Minor. Mineral Research and Exploration Bulletin 66, 20–34.

Kurt, H., 1994. Petrography and geochemistry of Kadinhani (Konya) area, Central Turkey. Unpublished PhD thesis, Glasgow University, UK, 191 pp.

Kurt, H., 1996. Geochemical characteristics of the metaigneous rocks near Kadinhani (Konya), Turkey. Geosound 28, 1–21.

Kurt, H., Eren, Y., 1998. Petrographical and geochemical characteristics of metacarbonates in the Bozdag Formation, northwest Konya. Goldschmidt Conference, Toulouse. Mineralogical Magazine 62A, 834–835.

Okay, A.I., 1984. Distribution and characteristics of the north–west Turkish blueschists. In: Robertson, A.H.F., Dixon, J.E. (Eds.), The geological evolution of the eastern Mediterranean. Geological Society of London Special Publication 17, 455–466.

Okay, A.I., 1986. High-pressure/low temperature metamorphic rocks of Turkey. In: Evans, B.V., Brown, E.H. (Eds.), Blueschists and Eclogites: Boulder, CO, Geological Society of America Memoir 164, 338–348.

Oktay, F.Y., 1982. Stratigraphy and geological evolution of Ulukisla and its surroundings. Geological Bulletin of Turkey 25, 15–24.

Özcan, A., Göncüoglu, M.C., Turhan, N., Uysal, S., Sentürk, K., Isik, A., 1988. Late Paleozoic evolution of the Kütahya-Bolkardagi belt. METU Journal of Pure and Applied Science 21 (1/3), 211–220.

Özcan, A., Göncüoglu, M.C., Turhan, N., Sentürk, K., Uysal, S., Isik, A., 1990. Geology of the basement rocks of the Konya–Kadinhani–Ilgin region. Mineral Research and Exploration Report No. 9535 (in Turkish, with English abstract).

Powell, C. McA., 1979. A morphological classification of rock cleavage. In: Bell, T.H., Vernon, R.H. (Eds.), Microstructural processes during deformation and metamorphism. Tectonophysics 58, 21–34.

Ramsay, J.G., 1967. Folding and Fracturing of Rocks, 568. McGraw-Hill, New York (568 pp.).

Sengör, A.M.C., 1984. The Cimmeride orogenic system and the tectonics of Eurasia. Geological Society of America Special Paper 195, 74.

Sengör, A.M.C., Yilmaz, Y., 1981. Tethyan evolution of Turkey: a plate tectonic approach. Tectonophysics 75, 81–241.

Sengör, A.M.C., Yilmaz, Y., Sungurlu, O., 1984. Tectonics of the Mediterranean Cimmerides: nature and evolution of the western termination of Palaeo-Tethys. Geological Society of London Special Publication 14, 117–152.

Wiesner, K., 1968. Konya mercury deposits and studies on them. Mineral Research and Exploration Bulletin 70, 178–213 (in Turkish).